https://doi.org/10.5194/acp-2020-551
Preprint. Discussion started: 24 August 2020

Atmospheric Chemistry and Physics Discussions

Occurrence of discontinuities in the ozone concentration data from three reanalyses

Peter Krizan, Michal Kozubek, Jan Lastovicka

Institute of Atmospheric Physics, Czech Academy of Sciences, 14100 Prague, Czech Republic;

Correspondence: Peter Krizan (krizan@ufa.cas.cz)

Abstract

Ozone is a very important trace gas in the stratosphere and thus we need to know its temporal evolution over the globe. The ground based measurements are rare, especially in the Southern Hemisphere. Satellite ozone data have broader coverage, but they are not available from everywhere. On the other hand, the reanalyse data have regular spatial and temporal structure, which is very good for trend analyses. But there are discontinuities in these data. These discontinuities may influence the results of trend studies. The aim of this paper is to detect the discontinuity occurrence (DO) in the following reanalyses: MERRA-2, ERA5 and JRA-55 with the help of the Pettitt homogeneity test at all common layers above 500 hPa. The discontinuities are sorted according to their size to the significant and the insignificant ones; the former can affect the ozone trend studies. It was shown that DO for the significant discontinuities is the smallest in JRA-55. In the upper model layers, the discontinuity occurrence is the highest. The other area of high DO is the troposphere.

1. Introduction

Ozone is an important trace gas in the atmosphere, because it protects the biota of the Earth from the harmful ultraviolet radiation. In the beginning of the 1970s the ozone research was mostly interested in the connection between the ozone layer and the supersonic transport. The great challenge was the discovering of the Antarctic ozone hole. The origin of the ozone hole is in the chemical reactions of anthropogenic halogen radicals, which destroy ozone (Solomon, 1999). As a consequence of these results, the Montreal Protocol and its amendments was signed, which stopped the production of the ozone-depleting substances (ODS). This protocol led to a decrease of ODS concentrations in the stratosphere (WMO, 2014). There are some signs of the ozone layer recovery, especially in the upper stratosphere (Harris et al., 2015). In addition, all models predict the future recovery of the ozone layer (Eyring et al., 2010). The concentration of ODS is not the only factor that has impact on the ozone layer. In addition, the greenhouse cooling of the stratosphere (Waugh et al., 2009) and changes in the Brewer–Dobson circulation influence the ozone concentration. In such situation, proper trend analysis is necessary for the understanding of the ozone layer behaviour. Trend analyses based on ground-based data (Mc Landress et al., 2009; Krzyscin et al., 2008) suffer with data being measured at single locations only, and the number of ground-based stations is insufficient, especially in the Southern Hemisphere. Satellite ozone data have broader coverage, and these data are widely used in trend analysis in the ozone research (e.g., Jones et al., 2009). In order to have long data series of satellite ozone measurements, composites from various satellites have been used (e.g., Ball et al., 2019; Bourassa et al., 2014; Tummon et al., 2014). But in some areas, it is impossible to measure ozone (polar night, below dense clouds) by satellite. SPARC Report No. 9 (2019) critically summarizes the current state-of-the-art as concerns trends in stratospheric ozone.

https://doi.org/10.5194/acp-2020-551
Preprint. Discussion started: 24 August 2020

Atmospheric Chemistry and Physics Discussions

On the other hand, the ozone data from reanalysis are generated in equal time step and they are spatially homogeneous, but there is a big question of the suitability of these data for trend analysis due to the occurrence of discontinuities (Bengtsson et al., 2004). They can be caused by satellite or instrument replacements or by the assimilation of not homogenous basic parameters. Shangguan et al. (2019) considered the evaluation of trends from reanalysis and found some problems with the homogeneity of this type of data. Occurrence of the artificial discontinuities is a great problem in trend studies based on reanalyse data, because their occurrence artefacts the value of ozone trends and their significance. Only the artificial discontinuities are problematic, not the real ones. To our best knowledge there are no real discontinuities in ozone time series of monthly data so the majority of discontinuities is artificial.

Krizan et al. (2019) searched for the discontinuities in MERRA-2 ozone data. The aim of our paper is to extend this analysis to the ERA5 and JRA-55 data and compare the results from all three reanalyses. We use standard Pettitt homogeneity test (Pettitt, 1979) for all reanalyses in the period 1980–2017. Our study can help us to compare the data quality in these reanalyses as a first step toward to the trend studies. This paper is divided into the following sections: Section 2 describes the data and method, Section 3 provides results, Section 4 discusses the results, and Section 5 contains conclusions.

2. Data and method

At first we must explain the Pettitt homogeneity test.

Figure 1 and Table 1 present the artificial time series, which consists of part with no trend (from member 1 to 5) and part with the negative trends (from member 6 to 10). They model the onset of Antarctic ozone hole. Above member 10 we repeat the series and we add 10 to each member to get a discontinuity. So we have series of the length 20 and with discontinuity. Then the series is sorted in ascending order. The results are given in the second row of Table 1. Now we look at the first element in the second row: it is 1, 1 is the 10^{th} element of the series (row 1) and this value is the first element in row 3 of Table 1. Similarly, the second element of the row 2 is 3, it is the 9^{th} element of artificial series and this number is the second element of the row 3 in Table 1. When this procedure is done for all elements of the series, we obtain the third row of Table 1. Then we perform the cumulative sum of row 3. The results are given in row 4 of Table 1. Let X_i is the i^{th} element of this cumulative sum. The value U_i is defined as follows:

$$U_i = \text{abs}\,(2X_i - i(l+1)) \quad (1)$$

Where abs is the absolute value and l is the length of series (in our case l = 20). The values U are given in the last row of Table 2. Now we find the maximal value of U from Table 1. It is 81 and it is the 11^{th} element of U series. In next step we must compute the characteristics p is calculated:

$$P=e^{T} \quad (2)$$

where $$T= -6(\max(U))^2/(l^3+l^2) \quad (3)$$

https://doi.org/10.5194/acp-2020-551
Preprint. Discussion started: 24 August 2020

Atmospheric Chemistry and Physics Discussions

where l is the length of series. If P< 0.05 the discontinuity is detected at the element of series where U is maximal, otherwise the discontinuity is not detected according the Pettitt (1979). In our case max(U)=81, l=20 so T=-4.69 and P=0.0092. 0.0092<0.05 so the discontinuity is detected at element 11 of the series. The 11th element is the right element where the discontinuity occurs (vertical red line in Figure 1 and first row in Table 2). So the Pettitt test is able to detect the discontinuity, but it does not detect discontinuity where negative trends in time series starts (element 5 and 16). So this procedure will not wrongly detect the onset of ozone hole as a discontinuity. We also did some simulations concerning the behaviour of this test in the cases when the discontinuity occurs at the edge of the series. When the discontinuity was present at every element up to the 18th one, this test was able to detect it

In this paper, we used the ozone monthly means from MERRA-2, ERA5 and JRA-55 above 500 hPa in the period 1980–2017. Table 2 shows that the top layer in the reanalyses is not the same for various reanalyses: The top modelling level for JRA 55 is 0.1 hPa and for MERRA-2 and ERA5 0.01 hPa. However, the top available/published level for all parameters is 1 hPa (JRA-55 and ERA5) and 0.1 hPa (MERRA-2). The layers 4 hPa and 40 hPa are present only in MERRA-2 and the data from 125 hPa, 175 hPa and 225 hPa are given only in ERA5 and JRA-55, not in MERRA-2. Reanalyses used in this paper cover the whole satellite era. They include substantial upgrades and changes to the data assimilation system and input data. We choose these three reanalyses because they are mostly used in atmospheric community and they are the newest ones at this time. In MERRA-2 new constraints are applied to ensure the conservation of global dry-air mass and to close the balance between surface water fluxes (precipitation minus evaporation) and changes in total atmospheric water (Takacs et al., 2016). The modified gravity wave scheme substantially improves the model representation of the quasi biennial oscillation (Molod et al., 2015; Cog et al., 2016). The assimilation of Microwave Limb Sounder (MLS) temperature retrievals at high-pressure levels (lower than 5 hPa) should improve the reanalysis at upper levels. The assimilation of MLS stratospheric ozone profiles and Ozone Monitoring Instrument (OMI) column ozone since the beginning of the Aura mission in late 2004 also improve the representation of fine-scale ozone features, especially in the region around the tropopause (Randles et al., 2016). MERRA and MERRA-2 use the Three Dimensional Variational (3D VAR) assimilation process. MERRA-2 uses regular latitude–longitude grids from 1000 to 0.01 hPa (1/2° latitude × 5/8° longitude). The warm bias in the upper troposphere has gradually been decreasing because the observing system has been improving. A change in observing systems occurred in July 2006, when the GNSS-RO refractivities were included into JRA-55. The impact of changes in observing systems on the JRA-55 time series is reduced compared with JRA-25 but the low-frequency variations are smaller than those of the SSU datasets, especially in the upper stratosphere (Kobayashi et al., 2015). Three-dimensional daily mean ozone distributions are implemented in JRA-55 for the period after 1979. It was produced separately from the JRA-55 data assimilation system using the T42L68 resolution version of the chemistry climate model (CCM) developed at the Meteorological Research Institute (MRICCM1, Shibata et al., 2005). According to Harada et al. (2016) the JRA-55 reanalysis well represent the general features of the QBO and SAO. JRA-55 has also reduced biases in the lower stratosphere compared with JRA-25 except the northern polar region. JRA-55 uses the Four Dimensional Variational (4D VAR) assimilation process. JRA-55 uses regular latitude–longitude grids from 1000 to 0.1 hPa (0.562° latitude x 0.562 longitude). Detail description of all reanalyses (included JRA-55 and MERRA 2) can be found in Fujiwara et al. (2017) and Gelaro et al. (2017). ERA5 uses 4D-Var data assimilation in CY41R2 of ECMWF's Integrated Forecast System (IFS), with 137 hybrid sigma/pressure (model) levels in the vertical, with the top level at 0.01 hPa (0.25° latitude x 0.25 longitude). Atmospheric data are interpolated to 37 pressure levels up to 1 hPa. From 2000 to 2006, ERA5 has a poor fit to radiosonde temperatures in the stratosphere, with a cold bias in the lower

https://doi.org/10.5194/acp-2020-551
Preprint. Discussion started: 24 August 2020

Atmospheric Chemistry and Physics Discussions

stratosphere. In addition, a warm bias higher up persists for much of the period from 1979. More details about ERA5 can be found in CDS (2017).

We did our analysis for each grid point. Spatial (longitudinal and latitudinal) averages are not used, because during every averaging some information is lost. In each grid and each layer, we used the time series of the ozone concentration and applied the Pettitt homogeneity test to look for discontinuity in it. In each grid, the Pettitt test estimates only one main (biggest) discontinuity, so this procedure is not able to detect multiple discontinuities. This test is widely used in the climatological research especially for precipitation and temperature analysis (Javari, 2016; Firat et al., 2010; Wijngaard et al., 2003; Kozubek et al, 2020). We are interested primarily in the spatial distribution of the discontinuities. In each layer and month, we constructed the map of discontinuity occurrence. The Pettitt test tells us the year in which the discontinuity in time series occurs. But it does not say how big the discontinuity is or how it can affect trends. Small discontinuities have little impact on the trend analyses. On the other hand, a large discontinuity can have a strong trend impact, so we must divide the discontinuities according to their size. We tried to identify which ones were significant (in our case big enough to impact the trend) or insignificant according to this rule: Suppose we have a time series with the length L, and let in year x, the discontinuity occurs. We compute the difference between the average before the year x and after this year. If this difference is larger than the variance of time series, we can say that the discontinuity is significant and could have impact on trends, and we should be careful using this grid point in a trend analysis.

3. Results

For each layer and each reanalysis we compute the average, maximal and minimal DO from all months and the results are given in Figure 2 (3) which shows the vertical profiles of the average, minimal and maximal discontinuity occurrence for MERRA-2 (upper panel), ERA5 (middle panel) and JRA-55 (lower panel) for all (significant) discontinuities. The percentage shown in Figures 2 and 3 means how many of all grid points at a given level contain discontinuities, and this is shown for all levels in the form of profile. These profiles enable us to compare discontinuity occurrence (DO) among the reanalyses. In Figures 2 and 3 there are layers where the discontinuities are present more frequently or less frequently.

3.1. Comparison of the discontinuity occurrence between MERRA-2 and ERA5

3.1.1. All cases

The average DO from each month and each common layer is shown in Figure 4 for MERRA-2 and ERA5 for all discontinuities (upper panel). The sign S in the figures means the difference between the average DO from MERRA-2 and ERA5 is statistical significant at the 95 % level. The maximal DO for MERRA-2 occurs at 1 hPa (93,4 %) and minimal at 20 hPa (24,9 %). The other area of high DO is the troposphere with maximum 85,2 % at 400 hPa. The ERA5 average DO have also maximum in the upper stratosphere (98,5 % at 2 hPa), sharp minimum at 5 hPa (25,0 %) and the high DO is observed in the troposphere with maximum 70,4 % at 350 hPa. Above 350 hPa the average DO is higher at the majority of layers for ERA5. The only statistically significant differences between the average DO is seen at 2, 3 and 250 hPa. On the contrary below 350 hPa we observe higher average DO for MERRA, but these differences are not significant.

Table 3 presents the average DO difference between MERRA-2 and ERA5 for each month and each common layer for all discontinuities (left columns). When the differences are

https://doi.org/10.5194/acp-2020-551
Preprint. Discussion started: 24 August 2020


Atmospheric Chemistry and Physics Discussions

positive it means DO is larger in MERRA-2 than in ERA5. The opposite is true for the negative ones. All differences above 1 % in absolute value must be regarded as significant, because the number of grids is very high (1038240 for ERA5 and 207936 for MERRA-2). The DO differences are similar at the same layer and some layers have larger differences than others. At 2 and 3 hPa we see larger and significant negative DO differences. This means the DO is larger in ERA5 than in MERRA-2. The variance of DO is at some layers high, so it is the reason why the differences between MERRA-2 and ERA5 are insignificant at the majority of layers.

We can look at the differences in the distribution of discontinuities for areas where the DO differences are significant. We display the results only for month with the highest difference so we must compare the panels within one figure, not among figures. Figure 3 (upper panel) reveals two main areas of significant DO differences: upper stratosphere and 250 hPa. Figure 5 shows the geographical distribution of discontinuities at 3 hPa for September (difference -67.9 %) for MERRA-2 (upper panel) and for ERA5 (lower panel). The yellow colour means there is no discontinuity in a given grid and the red one shows the discontinuity in a given grid. MERRA-2 displays the majority of grids with no discontinuity, while for ERA5 discontinuities occur for large number of grids. At the 250 hPa level (FigureS1 in supplement) the geographical distribution is similar (difference is smaller -41.5 %, April).

3.1.2. Significant cases

Figure 4 shows the average DO from each month and each common layer also for the significant discontinuities (lower panel). The vertical profile of DO has similar shape as in the case of all discontinuities. MERRA-2 has maximal DO at 1 hPa (86.1 %) and minimal at 7 hPa (1.5 %). The ERA5 average DO has reached maximum in the upper stratosphere (87.7 % at 2 hPa) and sharp minimum at 5 hPa (8.4 %). The ERA5 average DO in the troposphere is much higher than for MERRA-2 with maximum 48.1 % at 350 hPa. In the case of the significant discontinuities at the majority of layers we observe higher average DO for ERA5 than for MERRA-2. The largest differences in the vertical profile pattern between all and the significant discontinuities is seen in the troposphere, where in the case of all discontinuities we see higher DO for MERRA-2 than for ERA5. The opposite is true for the significant DOs. The DO differences between MERRA-2 and ERA5 are significant in the upper stratosphere at 3 hPa and in the troposphere at 250, 300 and 350 hPa.

Table 3 gives the average DO differences between MERRA-2 and ERA5 for each month and each common layer for the significant discontinuities (right columns). The largest differences are seen at 3 hPa, where MERRA-2 DO is much smaller than that of ERA5. The negative differences are larger in absolute value for the significant discontinuities. In the troposphere we see positive differences in the case of all discontinuities and the negative ones for the significant discontinuities.

We can look at the differences in the geographical distribution of discontinuities for the selected cases where DO differences are significant. Figure 3 (lower panel) reveals two main areas of significant DO differences: the upper stratosphere and the troposphere. The geographical distribution of discontinuities at 3 hPa for June (difference -74.8 %) for MERRA-2 and ERA5 is shown in Figure 6. In the case of MERRA-2 the majority of grids reveal no discontinuity, while for ERA5 we observe discontinuities at a large number of grids. At 250 hPa (Figure S2 in supplement) the geographical distribution is similar (difference is smaller -49.1 %, May).

https://doi.org/10.5194/acp-2020-551
Preprint. Discussion started: 24 August 2020

Atmospheric Chemistry and Physics Discussions

3.2. Comparison of the discontinuity occurrence between MERRA-2 and JRA-55

3.2.1. All cases

The vertical profiles of DO for MERRA-2 and JRA-55 are seen in Figure 7 (upper panel). Above 10 hPa DO is higher for JRA-55 than for MERRA2 with significant differences at 3 and 5 hPa. Below 10 hPa DO from JRA-55 is smaller than from MERRA2 at all layers. Significant differences occur at 30 hPa and in the troposphere below 300 hPa, where difference in each layer is significant. These results are supported also by Table S1 in supplement, where the average monthly DOs are shown. These differences are negative above 10 hPa and positive below with maximal differences in the stratosphere at about 5 hPa and in the troposphere. For the majority of grids there are no discontinuities in the case of MERRA-2. The opposite is true for JRA-55. In the troposphere the situation is very different. Figure S3 in supplement displays the geographical distribution of DO at 400 hPa in March (difference 64.8 %). There is a discontinuity in the case of MERRA-2 (upper panel) at nearly all grids. DO is substantially lower for JRA-55 (lower panel).

3.2.2. Significant cases

In the case of the significant discontinuities (Figure 7, lower panel) we can observe at the majority of layers JRA-55 DO to be smaller than that of MERRA2. There are huge differences in behaviour of DO in the case of significant and all discontinuities in the uppermost layers (1 and 2 hPa). DO of all discontinuities is larger for JRA-55, the opposite is true for the significant discontinuities, where at 1 hPa the MERRA-2 versus JRA-55 differences are significant. From 3 hPa down to 10 hPa we observe insignificant differences with higher DO values for JRA-55. Below 10 hPa DO is higher for MERRA-2 at all layers, but these differences are insignificant except for 50 hPa. The monthly DO values are shown in Table S1 in supplement. At 1 hPa DO differences for all discontinuities are small and negative for nearly all months, while for the significant discontinuities these values are high and positive (DO is higher for MERRA-2). Similar DO patterns are seen at 2 hPa. From 3 hPa down to 10 hPa we observe small negative monthly DO values in agreement with Figure 7. Below 10 hPa DO values are positive for majority of months and layers. Figure 8 shows the geographical distribution of significant discontinuities at 1 hPa for October (difference 84.9 %). In MERRA-2 there are discontinuities at the vast majority of grids, while for JRA-55 the occurrence of discontinuities is strongly reduced.

3.3. Comparison of discontinuity occurrence between ERA5 and JRA-55

3.3.1. All cases

Figure 9 (upper panel) shows vertical profiles of the average DO for ERA5 and JRA-55 for all discontinuities. The profile patterns are similar as for MERRA-2 and JRA-55 DOs. Above 5 hPa DO for ERA5 is comparable or slightly higher than for JRA-55. At 5 hPa there is a sharp minimum in DO in the case of ERA5, so this difference is significant. Below 7 hPa DO for JRA-55 is smaller at all layers. These differences are significant from the lower stratosphere (below 225 hPa) down to the upper troposphere (above 500 hPa). These results are confirmed also by Table S2 in supplement, where monthly values of DO are shown. Above 5 hPa we observe small negative differences (DO in JRA-55 is higher). At 5 hPa these differences are the highest in absolute value. Below 7 hPa the differences are positive at the

https://doi.org/10.5194/acp-2020-551
Preprint. Discussion started: 24 August 2020


Atmospheric Chemistry and Physics Discussions

majority of layers and months. The geographical distribution of all discontinuities at 5 hPa for August (difference -83.3 %) reveals Figure 10 for ERA5 (upper panel) and for JRA-55 (lower panel). For JRA-55 the discontinuities occur at vast majority of grids, while for ERA5 the number of discontinuities is substantially lower. The situation is opposite in the troposphere (Figure S4 in supplement). At 250 hPa in June (difference 58.7 %) the occurrence of discontinuities is higher for ERA5 than JRA-55.

3.3.2. Significant cases

Figure 9 (lower panel) shows the average vertical profile of DOs for ERA5 and JRA-55 for the significant discontinuities. Again the vertical distribution of DOs is similar to that for MERRA-2. At all layers except 5 hPa the discontinuity occurrence is higher for ERA5 than JRA-55. These differences are significant above 3 hPa, at 50 and 70 hPa and at all layers below 225 hPa. These conclusions are in agreement with the results of Table S2 in supplement, where at the majority of months and layers we see positive differences, which means DO is higher for ERA5 than JRA-55. Figure 11 (2 hPa, June difference 91.6 %) and Figure S5 in supplement (400 hPa, December, difference 54.7 %) also support these conclusions.

4. Discussion

The vertical profile of DO is similar at each month within one reanalysis, which means it is reasonable to compare the DO profiles among the reanalyses. There are layers at which DO is higher (lower) than at the others and these layers are the same for each month within one reanalysis. In general, DO is higher in the upper stratosphere and the other area of the high DO is in the troposphere. The errors of satellite measurements increase in the lowest stratosphere and in the troposphere, where the most important measurements are those from the sondes, but they are pointwise. When the amount of data is lower, the changes in data amount or changes in measurement techniques have greater impact on the reanalysis result and on discontinuity occurrence, which might be the reason for the tropospheric increase of DO.

Now we discuss the results of comparing the discontinuity occurrence for each pair of reanalyses. When we look at the DO in the uppermost layers we see DO for MERRA-2 is lower than those of ERA5 and JRA-55 for all discontinuities. Discontinuity occurrence is very high at about 1 hPa at all three reanalyses. MERRA-2 has also lower DO for significant discontinuities than ERA5 in these layers. It is very interesting DO for the significant cases is lower for JRA-55 than that for MERRA-2 and ERA5 above 5 hPa.

MERRA-2 and ERA5 have the same top model layer (0.01 hPa), but for ERA5 the top model layer available for public is 1 hPa. ERA5 and JRA-55 use the same assimilation procedure (4D VAR), while MERRA-2 uses 3D VAR procedure. The differences in upper stratosphere, which means around top of all reanalyses, are one of the main problem which should be studied in more details. This region is very important for vertical coupling in the middle atmosphere. DO differences among the reanalyses could be affected by differences in data used in these reanalyses. On the other hand, amount of observations in this region is very low compared to lower pressure levels, which contributes to large DO in the upper stratosphere. That is why assimilation procedure and used models can play important role. Due to combination of different assimilation procedure, not ideal satellite and homogenous observations and complicated modelling processes it is very difficult to identify the main problem.

https://doi.org/10.5194/acp-2020-551
Preprint. Discussion started: 24 August 2020

Atmospheric Chemistry and Physics Discussions

Another area of DO differences is the troposphere. Occurrence of all discontinuities is higher for MERRA-2 than for ERA5, but for the significant discontinuities, DO is much higher for ERA5 than for MERRA-2. It means there are more insignificant discontinuities in MERRA-2 than in ERA5, but the opposite is true for the significant ones. For trend analyses the significant discontinuities have larger impact on result, so the ERA5 data in the troposphere is more suitable for trend analysis than that of MERRA-2. DO values from JRA-55 are the smallest from all three reanalyses at each layer below 10hPa for all and the significant discontinuities. So the JRA-55 is the most suitable for ozone trend analyses from all three analyses due to small number of significant discontinuities, which affect the trend results.

It is necessary to focus on the connection between the results of this paper and future trend analyses. The greatest impact on trend results has got the presence of the significant discontinuities in the time series. According to our results the number of these significant discontinuities is the lowest in the JRA-55. This number is higher in MERRA-2 and ERA5 and it is comparable between these two reanalyses. If one wants to explore reanalysis data for trend analyses, it is necessary to look at the correlation between the trend patterns and patterns of discontinuity occurrence. If the correlation is present, the discontinuity influence must be taken into account. It will be interesting to look at the discontinuity occurrence in the total ozone time series from reanalyses, because we did this analyses for the ozone concentration time series from each layer, not for total ozone. It is reasonable to suppose the results might be partly different.

Wargan et al. (2018) used three different MERRA-2 assimilation and model products and found downward lower stratospheric ozone trends from 1998 to 2016 similar to satellite-based observational trends by Ball et al. (2018).

A significant change to the MERRA-2 meteorological assimilation occurred in 1998 with the launch of ATOVS (Long et al., 2017) onboard NOAA-15. The changes associated with new ATOVS data are also evident in other reanalysis systems (e.g., ERA-Interim and JRA-55; Long et al., 2017). 1998-1999 has been identified as the period of greatest change to reanalysis meteorology in the middle atmosphere (Fujiwara et al., 2017).

In our paper we were not interested in temporal occurrence of discontinuities. According to Shangguan et al. (2019) the first period of ozone discontinuity presence is about 2003 when MERRA-2 switched from SBUV to MLS and the other in 2015 when MERRA-2 and ERA5 started to use 4.2 MLS data instead of version 2.2. Similar result for MERRA-2 was obtained by Krizan et al. (2019).

5. Conclusions

The occurrence of discontinuities in series of ozone concentration data at various stratospheric and tropospheric levels between 500 and 1 hPa were searched for three modern reanalyses ERA5, MERRA-2 and JRA-55. This study is based on analysis of data in individual grid points, not on zonal or other averages. The obtained results have implications for usability of ozone data from reanalyses for trend studies. The main results of this paper are as follows:

- There are differences in the discontinuity occurrence frequency among reanalyses.
- In the upper stratosphere we observed the tendency toward the higher discontinuity occurrence in all reanalyses
- Another area of higher discontinuity occurrence is the troposphere

https://doi.org/10.5194/acp-2020-551
Preprint. Discussion started: 24 August 2020

Atmospheric Chemistry and Physics Discussions

- The discontinuity occurrence in JRA-55 is on average the lowest from all three reanalyses below 10 hPa, especially for the significant discontinuities.
- According to our results, JRA-55 is the most suitable for reanalyse trend studies due to the low significant discontinuity occurrence.

The follow-on investigations should focus on a similar investigation of discontinuity occurrence in the total ozone from reanalyses and on application of reanalyses data for long-term trend studies.

Acknowledgements

ECMWF, NASA and Japanese Meteorological Society are acknowledged for development of ERA5, MERRA-2 and JRA-55 and for possibility to use these data.

Author Contributions: This paper was prepared in close collaboration of all authors but the major part of the work was done by Peter Krizan.

Competing interests: The authors declare no conflicts of interest.

Financial support: Support by the Czech Science Foundation via Grant 18-01625S is acknowledged.

Data availability:

ERA5: https://cds.climate.copernicus.eu/cdsapp#!/home

JRA-55: https://rda.ucar.edu/datasets/ds628.0/#access

MERRA2: https://cmr.earthdata.nasa.gov/search/concepts/C1276812931-GES_DISC.html

References

Ball, W. T., Alsing, J., Mortlock, D. J., Staehelin, J., Haigh, J. D., Peter, T., Tummon, F., Stubi, R., Stenke, A., Anderson, J., Bourassa, A., Davis, S. M., Degestein, D., Frith, S., Froidevaux, L., Roth,C., Sofieva, V., Wang, R., Wild, J., Yu, P. Ziemke, J.R. and Rozanov, E.V.: Continuous decline in lower stratospheric ozone offsets ozone layer recovery. Atmos. Chem. Phys., 18(2), 1379–1394, https://doi.org/10.5194/acp-18-1379-2018,2018

Ball, W.T., Alsing, J., Staehelin, J., Davis, S.M., Froidevaux, L., and Peter, T.: Stratospheric ozone trends for 1985-2018: sensitivity to recent large variability, Atmos. Chem. Phys., 19, 12731-12748, https://doi.org/10.5194/acp-19-12731-2019, 2019.

Bengtsson, L., Hagemann, S., and Hodges, K.I.: Can climate trends be calculated from reanalysis data? J. Geophys. Res. Atmos. 2004, 109, D11111, doi:10.1029/2004jd004536, 2004.

Bourassa, A. E., Degenstein, D. A., Randel, W. J., Zawodny, J. M., Kyrölä, E., McLinden, C. A., Sioris, C. E., and Roth, C. Z.: Trends in stratospheric ozone derived from merged SAGE II and Odin-OSIRIS satellite observations, Atmos. Chem. Phys., 14, 6983–6994, doi:10.5194/acp-14-6983-2014, 2014.

https://doi.org/10.5194/acp-2020-551
Preprint. Discussion started: 24 August 2020

Atmospheric Chemistry and Physics Discussions

Copernicus Climate Change Service (C3S): ERA5: Fifth generation of ECMWF atmospheric reanalyses of the global climate. Copernicus Climate Change Service Climate Data Store (CDS) date of access. https://cds.climate.copernicus.eu/cdsapp#!/home,2017.

Coy, L., Wargan, K., Molod, A.M., McCarty, and W.R., Pawson, S.: Structure and dynamics of the quasi-biennial oscillation in MERRA-2, J. Clim. 29, 5339–5354, doi:10.1175/JCLI-D-15-0809.1, 2016.

Eyring, V., Cionni, I., Bodeker, G.E., Charlton-Perez, A.J., Kinnison, D.E., Scinocca, J.F., Waugh, D.W., Akiyoshi, H., Bekki, S., Chipperfield, M.P., Dameris, M., Dhomse, S., Frith, S.M., Garny, H., Gettelman, A., Kubin, A., Langematz, U., Mancini, E., Marchand, M., Nakamura, T., Oman, L.D., Pawson, S., Pitari, G., Plummer, D.A., Rozanov, E., Shepherd, T.G., Shibata, K., Tian, W., Braesicke, P., Hardiman S.C., Lamarque, J.F.,Morgestern, O., Pyle, J., A., Smale D. and Yamashita, Y.: Multi-model assessment of stratospheric ozone return dates and ozone recovery in CCMVal-2 models, Atmos. Chem. Phys., 10, 9451–9472, doi:10.5194/acp-10-9451-2010, 2010.

Firat, M., Dikbas, F., Cem Koç, A., and Gungor, M.: Missing data analysis and homogeneity test for Turkish precipitation series, Sadhana, 35, 707–720, 2010.

Fujiwara, M., Wright, J.S., Manney, G.L., Gray, L.J., Anstey, J., Birner, T., Davis, S., Gerber, E.P., Harvey, V.L., Hegglin, M.I.,Homeyer, C.,R., Knox, J. A., Kruger, K., Lambert, A., Long, C. S., Martineau, P., Molod, A., Monge-Sanz, B. M., Santee, M. L., Tegtmeier, S., Chabrillat, S., Tan, D. G. H., Jackson, D. R., Polavarapu, S., Compo, G. P. Dragani, R., Ebisuzaki, W., Harada Y., Kobayashi, C., McCarty, W., Onogi, K., Pawson, S., Simmons, A., Wargan, K., Whitaker J. S. and Zou C. Z.: Introduction to the SPARC Reanalysis Intercomparison Project (S-RIP) and overview of the reanalysis systems, Atmos. Chem. Phys., 17, 1417–1452, doi:10.5194/acp-17-1417-2017, 2017.

Gelaro, R.W., McCarty, M.J., Suárez, R., Todling, A., Molod, L., Takacs, C.A., Randles, A., Darmenov, M.G., Bosilovich, R., Reichle, K., Wargan, K., Lawrence, C. Cullather, R., Draper, C., Akella S., Buchard, V., Conaty, A., Silva, A. M., Gu, W., Kim, G., Koster, R., Lucchesi, R., Merkova, D., Nielsen, J. E., Partyka, G., Pawson, S., Putman, W., Rieneker, M., Schubert, S. D., Sienkiewicz, M. and Zhao, B.: The modern-era retrospective analysis for research and applications, Version 2 (MERRA-2), J. Clim., 30, 5419–5454, doi:10.1175/JCLI-D-160758.1, 2017.

Harada, Y., H. Kamahori, C. Kobayashi, H. Endo, S. Kobayashi, Y. Ota, H. Onoda, K. Onogi, K. Miyaoka, and K. Takahashi: The JRA-55 Reanalysis: Representation of atmospheric circulation and climate variability, J. Meteor. Soc. Japan, 94, 269-302, doi:10.2151/jmsj.2016-015, 2016.

Harris, N.R.P., Hassler, B., Tummon, F., Bodeker, G.E., Hubert, D., Petropavlovskikh, I., Steinbrecht, W., Anderson, J., Bhartia, P.K., Boone, C.D., Bourassa, A., Davis, S. M., Degenstein, D., Delcloo, A., Frith, S. M., Froidevaux, L., Godin-Beekmann, S., Jones, N., Kurylo, M. J., Kyrola, E., Laine, M., Leblanc, S. T., Lambert, J. C., Liley, B., Mahieu, E., Maycock, A., Maziere, M., Parrish, A., Querel, R., Rosenlof, K. H., Roth, C., Sioris, C., Staehelin, J., Stolarski, R. S., Stubi, R., Tamminen , J., Vigouroux, C., Walker, K. A., Wang, H. J., Wild, J. and Zawodny, J. M.: Past changes in the vertical distribution of ozone—Part 3: Analysis and interpretation of trends, Atmos. Chem. Phys. 15, 9965–9982, doi:10.5194/acp-15-9965-2015, 2015.

Javari, M.: Trend and homogeneity analysis of precipitation in Iran, Climate, 4, *44*, 2016.

Jones, A., Urban, J., Murtagh, D.P., Eriksson, P., Brohede, S., Haley, C., Degenstein, D., Bourassa, A., von Savigny, C., Sonkaew, T., Rozanov, E., Bovensmann, H. and Burrows, J..: Evolution of stratospheric ozone and water vapour time series studied with satellite measurements, Atmos. Chem. Phys. 9, 6055–6075, doi:10.5194/acp-9-6055-2009, 2009.

https://doi.org/10.5194/acp-2020-551
Preprint. Discussion started: 24 August 2020

Atmospheric Chemistry and Physics Discussions

Kobayashi, S., Y. Ota, Y. Harada, A. Ebita, M. Moriya, H. Onoda, K. Onogi, H. Kamahori, C. Kobayashi, H. Endo, K. Miyaoka, and K. Takahash: The JRA-55 Reanalysis: General specifications and basic characteristics. *J. Meteor. Soc. Japan*, **93**, 5-48, doi:10.2151/jmsj.2015-001, 2015.

Kozubek, M., Krizan, P. and Lastovicka, J.: Homogeneity of the temperature data series from ERA5 and MERRA2 and temperature trends. *Atmosphere*, *11*(3), 235, 2020

Križan, P., Kozubek, M. and Laštovička, J.: Discontinuities in the ozone concentration time series from MERRA-2 reanalysis, Atmosphere, 10, art. #812, doi: 10.3390/atmos10120812, 2019.

Krzyscin, J.W., and Borkowski, J.L.: Variabilty of the total ozone trend over Europe for the period 1950–2004 derived from reconstructed data, Atmos. Chem. Phys. 8, 2847–2857, 2008.

Long, C. S., Fujiwara, M., Davis, S., Mitchell, D. M., and Wright, C. J.: Climatology and interannual variability of dynamic variables in multiple reanalyses evaluated by the SPARC Reanalysis Intercomparison Project (S-RIP). Atmos. Chem. Phys., 17(23), 14593–14629, https://doi.org/10.5194/acp-17-14593-2017, 2017

McLandress, C.H., and Sheepherd, T.G.: Simulated anthropogenic changes in the brewer-dobson circulation, including its extension to high latitudes, J. Clim. 22, 1516–1540, doi:175/2008JCLI2979.1., 2009.

Molod, A., Takacs, L., Suarez, M., and Bacmeister, J.: Development of the GEOS-5 atmospheric general circulation model: Evolution from MERRA to MERRA2, Geosci. Model Dev., 8, 1339–1356, doi:10.5194/gmd-8-1339-2015, 2015.

Pettitt, A.N.: A non-parametric approach to the change point detection, Appl. Statist., 28, 126–135, 1979.

Randles, C.A., da Silva, A.M., Buchard, V., Darmenov, A., Colarco, P.R., Aquila, V., Bian, H., Nowottnick, E.P., Pan, X., Smirnov, A., Holben, B., Ferrare, R., Hair J., Shinozuka Y. and Flynn, C. J.: *The MERRA-2 aerosol assimilation, NASA Technical Report Series on Global Modeling and Data Assimilation, Volume 45*; NASA/TM-2016-104606; NASA Goddard Space Flight Center: Greenbelt, Maryland, 2016.

Shangguan, M., Wang, W. and Jin, S.: Variability of temperature and ozone in the upper troposphere and lower stratosphere from multi-satellite observations and reanalysis data, Atmos. Chem. Phys., 19, 6659–6679, doi:10.5194/acp-19-6659-2019, 2019.

Shibata, K., Deushi, M., Sekiyama, T.T. and Yoshimura, H.: Development of an MRI chemical transport model for the study of stratospheric chemistry. Pap. Geophys. Meteor., 55, 75–119, 2005.

Solomon, S.: Stratospheric ozone depletion: A review of concepts and history, Rev. Geophys., 37, 275–316, 1999.

SPARC Report N°9 (2019) of The SPARC LOTUS Activity: SPARC/IO3C/GAW Report on Long-term Ozone Trends and Uncertainties in the Stratosphere, eds. I. Petropavlovskikh, S. Godin-Beekmann, D.Hubert, R. Damadeo, B. Hassler, and V. Sofieva, SPARC Office, 10.17874/f899e57a20b, 2019.

Takacs, L.L., Suárez, M.J., and Todling, R.: Maintaining atmospheric mass and water balance in reanalyses, Q. J. Roy. Meteorol. Soc., 142, 1565–1573, doi:10.1002/qj.2763, 2016.

Tummon, F., Hassler, B., Harris N.R.P., Staehelin, J., Steinbrecht, W., Anderson, J., Bodeker, G. E., Bourassa, A., Davis, S. M., Degestein, D., Frith, S. M., Froidevaux, L., Kyrola, E., Laine, M., Long, C., Penckwitt, A. A., Sioris, C. E., Rosenlof, K. H., Roth, C., Wang, H. J. and Wild, J.: Intercomparison of vertically resolved merged satellite ozone data sets: interannual variability and long-term trends, Atmos. Chem. Phys., 14, 25687–25745, doi:10.5194/acpd-14-25687-2014, 2014.

Wargan, K., Orbe, C., Pawson, S., Ziemke, J. R., Oman, L. D., Olsen, M. A., Coy, L., and

https://doi.org/10.5194/acp-2020-551
Preprint. Discussion started: 24 August 2020

Atmospheric Chemistry and Physics Discussions

Knowland, K. E.: Recent decline in extratropical lower stratospheric ozone attributed to circulation changes. Geophys. Res. Lett., 45, 5166–5176. https://doi.org/10.1029/2018GL077406, 2018.

Waugh, D.W., Oman, L., Kawa, S.R., Stolarski, R.S., Pawson, S., Douglass, A.R., Newman, P.A. and Nielsen, J.E.: Impacts of climate change on stratospheric ozone recovery, Geophys. Res. Lett., 36, L03805, doi:10.1029/2008GL036223, 2009.

WMO. *Scientific Assessment of Ozone Depletion: 2014 Global Ozone Research and Monitoring Project Report*; World Meteorological Organization, Geneva, Switzerland, p. 416, 2014.

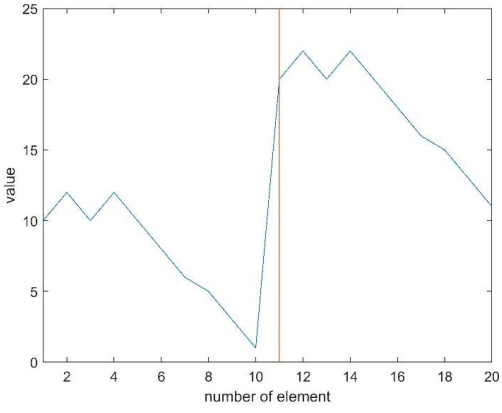

Figure 1 Artificial time series with discontinuity at element 11. The vertical red line is the resulting discontinuity searched for by Pettitt homogeneity test.

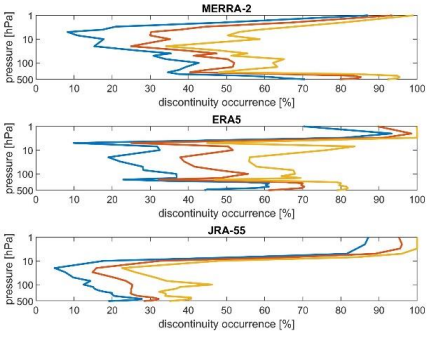

Figure 2 Vertical profiles of the minimal (blue), average (red) and maximal (orange) discontinuity occurrence for MERRA-2 (upper panel), ERA5 (middle panel) and JRA-55 (lower panel) for all discontinuities.

https://doi.org/10.5194/acp-2020-551
Preprint. Discussion started: 24 August 2020

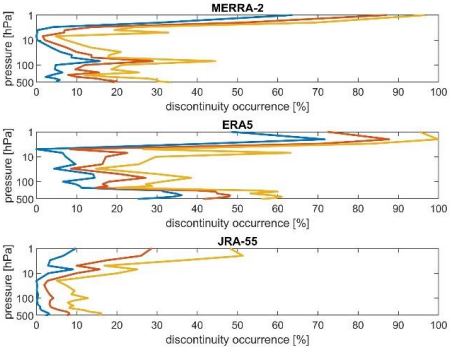

552

553 **Figure 3** The same as Figure 2 but for the significant discontinuities.

554

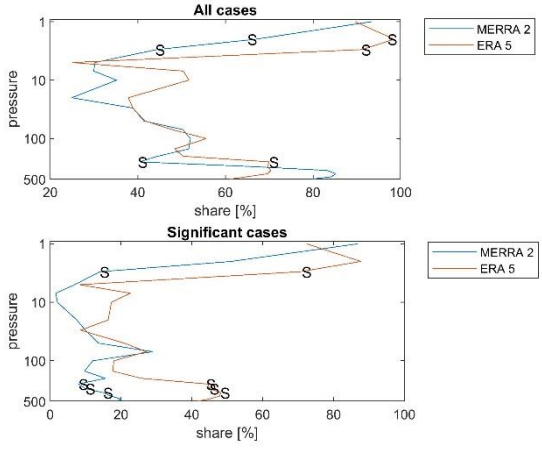

555
556

557 **Figure 4** The average vertical profile of DO for MERRA-2 and ERA5 for all (upper panel) and
558 significant discontinuities (lower panel). Letter S means significant difference between ERA5
559 and MERRA-2.

560

561

562

https://doi.org/10.5194/acp-2020-551
Preprint. Discussion started: 24 August 2020

Atmospheric Chemistry and Physics Discussions

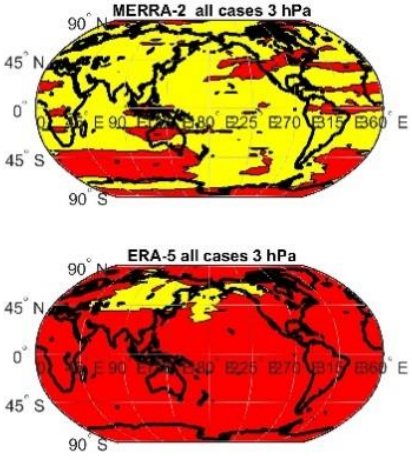

563

564 **Figure 5** Geographical distribution of all discontinuities (yellow – no discontinuity, red –
565 discontinuity) for MERRA-2 (upper panel) and ERA5 (lower panel) at 3hPa for September.

566

567

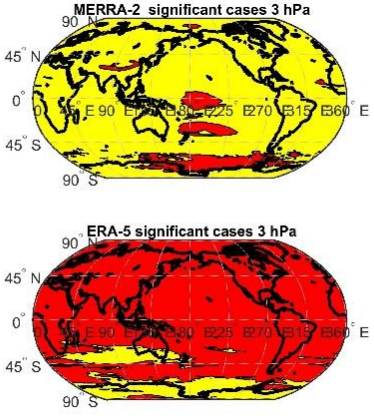

568
569 **Figure 6** Geographical distribution of the significant discontinuities for MERRA-2 (upper
570 panel) and ERA5 (lower panel) at 3hPa for June.

571

572

https://doi.org/10.5194/acp-2020-551
Preprint. Discussion started: 24 August 2020

Atmospheric Chemistry and Physics Discussions

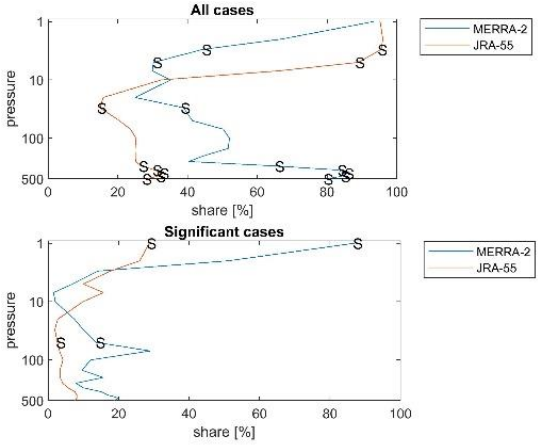

573
574
575 **Figure 7** The average vertical profile of DO for MERRA-2 and JRA-55 for all (upper panel)
576 and significant discontinuities (lower panel).

577

578

579

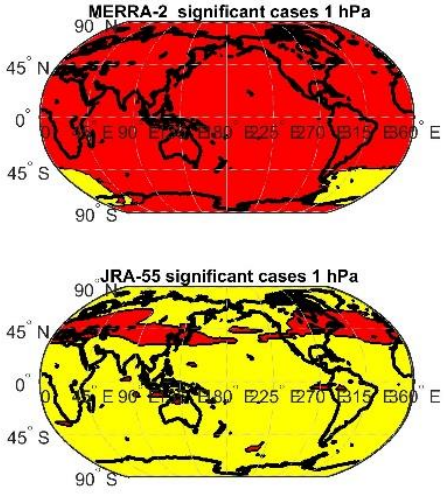

580
581 **Figure 8** Geographical distribution of the significant discontinuities for MERRA-2 (upper
582 panel) and JRA-55 (lower panel) at 1hPa for October.

583

584

585

https://doi.org/10.5194/acp-2020-551
Preprint. Discussion started: 24 August 2020

Atmospheric Chemistry and Physics Discussions

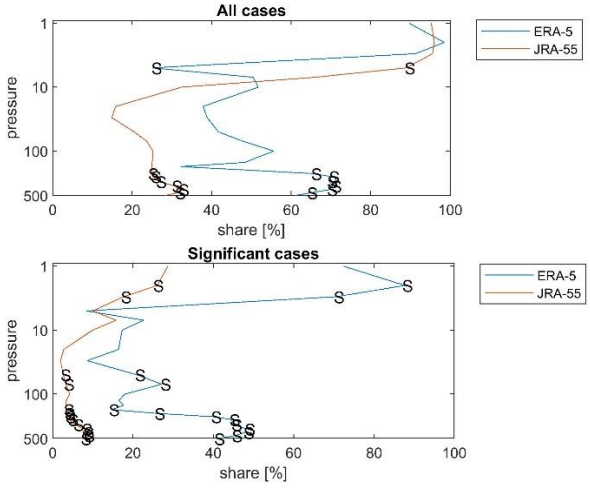

586

587

588 **Figure 9** The average vertical profile of DO for ERA5 and JRA-55 for all (upper panel) and
589 significant discontinuities (lower panel).

590

591

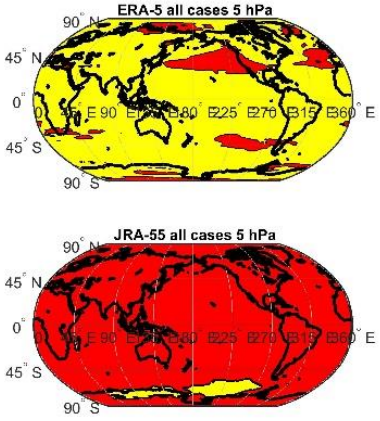

592

593 **Figure 10** Geographical distribution of all discontinuities for ERA5 (upper panel) and JRA-55
594 (lower panel) at 5hPa for August.

595

https://doi.org/10.5194/acp-2020-551
Preprint. Discussion started: 24 August 2020

Atmospheric Chemistry and Physics Discussions

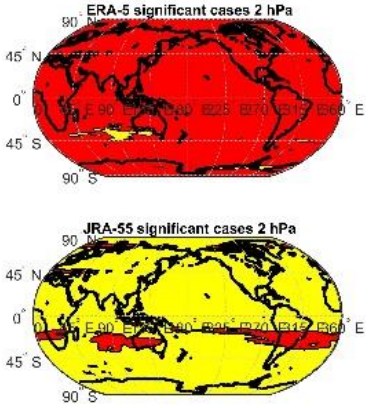

596
597 **Figure 11** Geographical distribution of the significant discontinuities for ERA5 (upper panel)
598 and JRA-55 (lower panel) at 2hPa for June.

599

600 **Table 1** Values which are needed for explanation of the Pettitt homogeneity test.

10	12	10	12	10	8	6	5	3	1	20	22	20	22	20	18	16	15	13	11
1	3	5	6	8	10	10	10	11	12	12	13	15	16	18	20	20	20	22	22
10	9	8	7	6	1	3	5	20	2	4	19	18	17	16	11	13	15	12	14
10	19	27	34	40	41	44	49	69	71	75	94	112	129	145	156	169	184	196	210
1	4	9	16	25	44	59	70	51	68	81	64	49	36	25	24	19	10	7	0

601

602 **Table 2** Layers in reanalyses used in this paper.

hPa	0,1	0,3	0,4	0,5	0,7	1	2	3	4	5	7	10	20	30	40	50
MERRA -2	*	*	*	*	*	*	*	*	*	*	*	*	*	*	*	*
ERA -5						*	*	*		*	*	*	*	*		*
JRA -55						*	*	*		*	*	*	*	*		*

603

hPa	70	100	125	150	175	200	225	250	300	350	400	450	500
MERRA -2	*	*		*		*		*	*	*	*	*	*
ERA -5	*	*	*	*	*	*	*	*	*	*	*	*	*
JRA -55	*	*	*	*	*	*	*	*		*	*	*	*

604

605

606

607

608

https://doi.org/10.5194/acp-2020-551
Preprint. Discussion started: 24 August 2020

Atmospheric Chemistry and Physics Discussions

609 **Table 3.** The differences in the discontinuity occurrence between MERRA-2 and ERA5 in
610 individual months for all (left column) and significant (right column) discontinuities. The
611 positive difference means higher number of discontinuities in MERRA-2 than in ERA5.

	January		February		March		April		May		June	
hPa	All	Sig.	All	Sig.	All	Sig.	All	Sig.	All	Sig.	All	Sig.
1	-2.3	8.5	28.5	39.4	11.3	25.5	10.5	7.8	-9.9	-7.2	3.2	-13.2
2	-25.2	-25.2	-51.2	-55.3	-39.8	-40.8	-28.1	-20.5	-19.6	-43.7	-29	-67.7
3	-37.4	-59.2	-47.1	-54.7	-65.0	-60.6	-40.9	-58.7	-39.0	-63.4	-38.6	-74.8
5	8.4	-11.0	18.9	24.4	22.9	0.2	-8.8	-9.7	-15.0	-17.1	-6.3	-0.4
7	14.6	-6.5	12.9	-16.7	-10.0	-19.7	-33.1	-10.2	-53.2	-37.4	-56.1	-62.7
10	1.1	-22.4	7.6	-20.7	9.0	-18.5	-27.4	-15.5	-31.4	-17.7	-29.5	-16.9
20	10.3	-1.6	-0.9	-9.3	-13.8	-1.1	-5.8	-5.7	-22.4	-11.8	-30.7	-20.1
30	4.0	0.5	7.2	0.2	2.3	2.5	-8.0	-3.0	-11.4	-5.6	-15.0	-2.6
50	-8.2	-5.1	5.4	0.0	4.3	-6.4	1.4	-11.4	12.5	-0.6	5.1	-12.0
70	5.7	0.9	13.2	1.8	5.0	5.1	8.8	7.9	10.8	17.5	7.1	14.9
100	-15.7	-7.3	-19.7	-9.7	-2.3	-2.8	5.9	-1.8	-8.0	-2.2	5.3	2.7
150	14.8	0.3	8.1	-5.1	-4.9	-7.1	1.7	-6.5	-11.6	-9.5	-4.7	-10.1
200	-4.5	-6.9	-0.1	-0.1	-11.6	-12.5	-13.8	-9.1	-17.3	-17.5	-9.1	-15.5
250	-22.2	-36.9	-24.6	-32.1	-39.1	-44.8	-41.5	-43.8	-40.2	-49.1	-40.2	-42.1
300	4.4	-30.1	7.9	-25.3	-9.0	-38.8	-6.8	-37.6	-12.7	-38.9	-32.9	-44.6
350	9.0	-29.0	22.7	-19.4	28.5	-29.1	30.9	-29.2	12.1	-38.1	-11.6	-44.3
400	14.5	-25.8	27.4	-16.5	35.7	-21.4	37.7	-28.1	12.0	-33.0	-7.1	-40.7
450	12.2	-21.5	18.4	-26.2	40.7	-15.9	38.9	-25.1	24.5	-14.2	5.3	-30.4
500	3.2	-30.7	11.3	-24.0	31.8	-11.6	29.9	-21.9	25.5	-7.2	23.7	-17.8

612
613
614
615
616
617
618
619
620
621
622
623
624
625

https://doi.org/10.5194/acp-2020-551
Preprint. Discussion started: 24 August 2020

Atmospheric Chemistry and Physics Discussions

626 Table3 continuation

	July		August		September		October		November		December	
hPa	All	Sig.	All	Sig.	All	Sig.	All	Sig.	All	Sig.	All	Sig.
1	2.8	18.9	-5.9	11.8	3.2	8.5	3.3	16.3	0.9	28.5	0.0	29.5
2	-39.7	-29.1	-26.3	-32.5	-22.7	-37.4	-17.8	-18.3	-34.8	-26.2	-45.5	-34.0
3	-47.6	-63.1	-63.4	-63.3	-67.9	-66.0	-50.0	-42.0	-34.6	-22.9	-30.4	-49.6
5	14.7	5.2	10.1	-0.1	-4.3	0.6	-2.3	-6.6	3.5	0.6	20.7	-3.5
7	-46.0	-39.5	-32.4	-28.0	-24.7	-11.2	-20.2	-6.0	-7.9	-9.9	10.6	-5.1
10	-37.7	-17.4	-29.3	-13.3	-16.4	-9.2	-21.7	-6.5	-11.3	-5.1	-10.9	-19.5
20	-35.3	-18.1	-30.1	-13.7	-8.7	-5.5	-6.0	-7.2	-10.0	-9.7	-1.3	-2.9
30	-14.1	-6.4	10.5	4.5	6.3	13.0	13.2	4.2	13.4	5.6	-7.9	3.2
50	0.4	-10.2	-4.9	-19.5	11.6	0.1	3.6	0.4	-15.1	-10.0	-19.4	-13.2
70	-3.2	6.0	-6.6	-6.1	-5.7	-7.0	1.5	0.7	0.6	-7.8	-7.9	-9.0
100	-1.9	-1.3	0.6	-21.0	2.1	-11.0	-3.8	-2.5	-1.2	-5.0	-4.9	-9.3
150	3.4	-3.5	-10.2	-23.3	-2.1	-18.0	16.4	-1.6	8.4	-9.4	19.0	-1.7
200	0.7	-1.3	5.3	-7.5	5.0	-16.8	-3.8	-12.0	-13.5	-12.9	-7.1	-10.8
250	-37.3	-34.1	-21.7	-29.5	-20.0	-27.7	-14.8	-21.4	-30.0	-42.9	-23.8	-35.6
300	-42.0	-47.3	-0.2	-34.5	2.8	-29.9	14.8	-25.8	17.3	-38.1	9.9	-29.3
350	-25.9	-53.6	14.6	-37.4	13.8	-34.5	22.0	-26.7	17.4	-31.0	17.9	-25.6
400	-10.5	-40.5	11.7	-36.4	15.3	-36.6	22.9	-29.9	13.6	-34.0	13.8	-27.6
450	14.7	-17.6	15.4	-23.9	13.4	-34.9	20.5	-29.7	13.1	-34.8	14.9	-25.9
500	24.7	-1.7	20.6	-16.4	10.6	-36.6	16.2	-28.6	9.9	-38.9	16.4	-34.6

627